Characterizing Protection Effects on Network Epidemics driven by Random Walks

Ronald C. de Souza[1], **Daniel R. Figueiredo**[1]

[1]Programa de Engenharia de Sistemas e Computação (PESC)
Universidade Federal do Rio de Janeiro (UFRJ)
Rio de Janeiro – RJ – Brazil

{rcsouza,daniel}@cos.ufrj.br

Abstract. Protection effects *(PFx) denote protective measures taken by individuals (such as to wear masks and wash hands) upon their risk perception towards an ongoing epidemic outbreak. The holistic force produced may fundamentally change the course of a spreading, with respect to both its reach and duration. This work proposes a model for PFx on network epidemics where nodes are sites mobile-agents may visit. Risk aversion is encoded as random walks biased to safe sites. Assuming the network is a complete graph, the model is analyzed and framed as a classical SIS. We find a regime under which PFx preclude endemic steady-states upon arbitrarily large rates for both walk and transmissibility. Simulation results support our theoretical findings.*

1. Introduction

The understanding on how epidemics either evolve and die out is increasingly pursued within various disciplines, for reasons such as to avoid potentially catastrophic impacts across society on its many spheres. In this context, *protection effects* (PFx) [Capasso and Serio 1978, Zhang et al. 2015], aka *disease-behavior dynamics* [Wang et al. 2015], denote the set of measures individuals take as to avoid contagion (such as to wear masks and wash hands), once aware that an epidemic unfolds nearby.

PFx fundamentally differ from *interventions*, which refer to epidemic-containment policies driven by governments: whereas interventions are carried out collective-to-individual (e.g. closure of schools, shops, restaurants, and flight cancellations [Amante and Balmer 2020, Cauchemez et al. 2011]), PFx arise as a behavioral product of individuals' danger-awareness; an individual-to-collective process. Indeed, intervention is typically encoded as a reduction in the number of contacts per unit time, possibly leading the epidemic to die out. PFx, in turn, are generally regarded as a kind of "saturation level" for the infection rate. Although conceptually different, both dynamics often express nonlinear forces acting against the spreading.

Recent studies have investigated how PFx may impact the course of an epidemic as predicted by traditional models. Most, however, elaborate over static, homogeneous-mixing standpoints. While mean-field approaches prove resourceful at capturing and elucidating many key aspects towards disease outbreaks, these also typically neglect, totally or partially, the structure of the underlying network of contacts and its time-varying nature as well.

This work investigates PFx in the context of network epidemics with mobile agents. Network nodes play the role of sites agents may visit, and protective behavior

comes from biasing their random-walks so these are prone to safe sites. Key-factors for modeling epidemics on mobile-agent setups include their spatio-temporal expressiveness. Indeed, to encode networks as topological structures mobile-agents transit upon is a natural way of capturing real-world mobility patterns [Draief and Ganesh 2011]. Models of this flavor have already been considered [Lam et al. 2012, Ibrahim 2012, Draief and Ganesh 2011, Tavares 2018]. To the best of our knowledge, however, PFx has hitherto never been investigated under such schemes; a gap filled in this paper.

Our main contributions are summarized as follows.

- A simple network epidemic model with mobile agents performing time-dependent biased random-walks to represent PFx. Agents' protective-behavior depends on their epidemic state—either susceptible (S) or infected (I).
- Assuming the network is a complete graph, a theoretical analysis using differential equations and the connection with the classical SIS model are both provided. The model predicts the onset of epidemics, and describes the endemic level as a function of model parameters.
- Characterization of the protective regime that leads to a disease-free steady state as a function of the model parameters. Moreover, even when the walk rate and transmissibility rate are arbitrarily large, a regime that precludes the epidemic is identified as a function of the other parameters.
- Design and implementation of a network epidemic simulator whose numerical results validate our model predictions.

The remainder of this paper is organized as follows. Section 2 discusses some representative works on PFx. Section 3 describes the proposed network epidemic model. PFx is then formalized in Section 4 and analyzed in Section 5. Section 6 support our analyses with simulation results. Finally, we conclude the paper with a brief discussion in Section 7.

2. Related Work

The compartmental approach proposed by Kermack & McKendrick (KMK) [Ogilvy et al. 1927] almost a century ago provided fundamental insights on the dynamics of susceptible-infected-recovered (SIR) epidemics, and inspired many models to be crafted on top of other compartment setups, notably SI, SIS and SIRS [Newman 2010].

Past roughly 50 years, [Capasso and Serio 1978] provided a generalization of KMK's model, replacing the (fixed) infection rate by an infection function $g(\cdot)$, thus capturing more complex—nonlinear—interactions between susceptible and infected agents. They show $g(\cdot)$ can play two different roles, namely intervention or protection effects. Their work is among the pioneers in considering such concepts as key-ingredients for predicting an epidemic's outcome.

Disease-behavior dynamics has ever since been investigated from many different perspectives [Wang et al. 2015, Funk et al. 2010]. For example, [Hyman and Li 1997] considers SIS epidemics of sexually-transmitted diseases. The authors formulate a mean-field model that segments population into risk-level groups, and conclude that behavioral changes (such as reducing contacts and partner formations) may decrease the infection

level. [Tchuenche et al. 2011] turns attention to the influence of local media on population's adaptive behavior to an ongoing outbreak, and conclude that media coverage does not necessarily help promoting epidemic containment. An intervened SIRS epidemic (i.e. a SIRS epidemic with intervention forces) [Cai et al. 2015] and a SIS epidemic with PFx (induced by media coverage) [Guo et al. 2018] were both investigated under Stochastic Differential Equations models. In both cases, it is shown that, even when the deterministic model predicts endemic regimes, the disease may still be suppressed in the presence of large random fluctuations. They hence conclude stochastic fluctuations may decisively change the course of such epidemics.

Risk awareness has also been analysed in the context of multiplex networks. For example, in [Granell et al. 2013] a network of physical interactions—through which an SIS epidemic spreads—is coupled to a (virtual) social-network wherein the same actors disseminate awareness in a fashion similar to an SIS epidemic. The authors show that the propagation of awareness may delay or even preclude epidemics that would, otherwise, yield large outbreaks. [Mao and Yang 2012] propose a framework for modelling PFx in multiplex networks and draw particular attention to the fact that real-world infection rates may be significantly larger than those predicted by models not encoding PFx.

When the time-varying nature of real-world contact patterns is taken into account, outbreaks may yield dynamics that both mass-action and static-network models fail to capture [Volz and Meyers 2007, Eames et al. 2012]. Within this paradigm, [Robinson et al. 2007] provides evidence that Great Britain's policies at the time adopted to restrict cattle movement between animal holdings in order to avoid disease outbreaks had gradually lost efficiency. Remarkably, the pointed reason is the self-organizing network induced by behavioral changes from farmers, who came to intensify cattle movement across the network's giant strong component. [Lee et al. 2012] shed light to the central role of temporal information for more efficient immunization strategies; PFx is not considered however. Particularly intriguing, [Zhou et al. 2012] provide insights on the protective dynamics that could possibly explain seasonal epidemics. Finally, [Yang et al. 2018] study the impacts of *emigration* as a protective maneuver. In their model, mobile agents are free to walk in any direction within a square region and move only upon imminent risk—choosing a new location uniformly at random. They conclude that protective actions performed sufficiently early may avoid endemic steady states.

None of these prior works, therefore, addresses PFx in epidemics where agents move within a network and locally avoid one another.

3. SIS epidemics with mobile-agents

We shall now describe the coupling of SIS epidemics with a mobile-agent environment, as considered in this paper. The following analysis—which still does not consider PFx—follows closely the work of [Ibrahim 2012] but has been modified in order to capture infections that depend on the exposure time interval. Table 1 lists the main symbols to be used throughout the text.

Mobility and contact pattern. Consider an undirected network $G = (V, E)$ with node and edge set given by V and E, respectively, where $n = |V|$ denotes its size. Consider a set K of $k = |K|$ agents, and let $v_j(t), j = 1, \ldots, k$ denote the location of agent j in time $t \geq 0$. Note that $v_j(t) \in V$ as agents can only be found in network nodes. At

Table 1. Symbols & terminologies

S-agents	Susceptible agents.
I-agents	Infected agents.
SI-contact	Contact (i.e. encounter) between an S-agent and an I-agent.
$G = (V, E)$	Undirected network wherein mobile-agents walk.
n	Network size, such that $n = \|V\|$.
$N(v)$	Set of neighbors of node v.
K, k	Set of agents, such that $k = \|K\|$.
$S(t), I(t)$	Set of S/I-agents at time t. $S(t) \cup I(t) = K$, $S(t) \cap I(t) = \emptyset$.
S, I	$\|S(t)\|$ and $\|I(t)\|$, respectively, thus $S + I = k$
s, i	S/k and I/k, respectively, hence $s + i = 1$.
i_0	Fraction of initially-infected agents, i.e. when $t = 0$.
τ	Disease transmissibility.
λ, β, γ	Walk rate, infection rate and recovery rate, respectively.
σ	Infection probability, such that $\sigma = \tau/(2\lambda + \tau)$.
α	SI-contact rate.
C	A constant, such that $C = (\tau k \lambda)/((2\lambda + \tau)n)$.
w_s	S-agent's tolerance to SI-contacts, $0 < w_s < 1$.
w_i	I-agent's tolerance to SI-contacts, $0 < w_i < 1$.

time zero, the location of an agent is chosen uniformly at random from V. Agents move according to continuous time random walks, where the residence time in any given node is exponentially distributed with rate $\lambda > 0$ (the walk rate). Once the agent has to move, it chooses its next node uniformly at random from the neighboring nodes (including its current node). Such transitions are assumed to occur instantaneously. Any two agents j and l are considered to be in contact one another *iff* both of them are located at the same node, $v_j(t) = v_l(t)$. Note that this leads to a dynamic *network of contacts* that is time-varying and can be characterized by a forest where every connected component is either a clique (representing those agents at one same site) or an isolated vertex (a single agent in a given spot).

Epidemic state and infection. Besides residing in a node, every agent has an epidemic state, denoted by "S" (susceptible) or "I" (infected). Let $c_j(t) \in \{$ "S","I" $\}$ denote the epidemic state of agent j at time $t \geq 0$. Also, let $S(t) = \{j \in K | c_j(t) =$"S"$\}$ and $I(t) = \{j \in K | c_j(t) =$"I"$\}$ denote the set of susceptible and infected agents at time t, respectively. Note that $S(t) \cup I(t) = K$ and $S(t) \cap I(t) = \emptyset$ for all t. Disease spreads through direct contact between an S-agent and an I-agent, with infection probability proportional to the duration of such a contact. The decision on whether or not an S-agent becomes infected is taken the moment it leaves its current node, as follows. Let t_e denote the total time an S-agent a remained exposed to one or more I-agents while residing in some node. Considering an exponential random variable Y with parameter $\tau > 0$, the probability that a becomes infected is simply $P[Y < t_e]$. The disease transmissibility thus depends on τ, such that within some fixed exposure interval an agent is more likely to become infected as τ gets larger.

Recovery. Note that agents can only become infected when taking a step, mov-

ing to some node. Once infected, an individual remains so for a certain time window, recovering right after. During such a period, however, the walker may infect others. The elapsed time until an agent recovers is assumed to be exponentially distributed with rate $\gamma > 0$—the recovery rate—, and independent of any other events.

As with other proposed random walk models [Draief and Ganesh 2011, Ibrahim 2012], a *sparse* scenario is assumed, where the number of nodes is much larger than the number of agents. In addition to being a good approximation for real-world sparse cases, this also allows the model to be simplified by assuming that only pairwise encounters occur, as the probability of having three or more agents in the same node becomes negligible. This assumption is fundamental for the following analysis.

3.1. Modeling the epidemic dynamics

The following deterministic model predicts the expected epidemic dynamics under the assumption that the network is a complete graph (i.e. a clique). As with the classical models, it relies on ODEs to capture the change in the population of S-agents and I-agents. In particular, dI/dt, the rate at which the number $I = |I(t)|$ of infected agents changes over time, depends on five different quantities (assuming $S = |S(t)|$ is the number of susceptible agents), as follows.

1. The rate at which two agents meet. Since G is a complete graph, this rate can easily be shown to be $2\lambda/n$, since their joint walk rate is 2λ and in one step they can reach any node $v \in V$.
2. The number of possible encounters among the agents. Since the sparse regime is assumed, only pairwise encounters are possible (with high probability), and thus there are a total of $\binom{k}{2}$ possible encounters;
3. The probability of an SI-contact. This is assumed to be number of possible SI-contacts at time t divided by the total number of possible contacts, and thus $SI/\binom{k}{2}$;
4. The probability of infection given an SI-contact, denoted by σ. This depends on the transmissibility τ and the total time the S-agent remained exposed, i.e. the duration of the SI-contact. Since both the contagion and the walking are governed by exponential random variables, it can be shown that

$$\sigma = \frac{\tau}{2\lambda + \tau}. \tag{1}$$

5. The total rate at which I-agents recover and become S-agents, which is simply given by γI, by independence among the agents in the recovery process.

Thus, the infected population dynamics is given by:

$$\frac{dI}{dt} = \binom{k}{2}\frac{2\lambda\sigma SI}{n\binom{k}{2}} - \gamma I = \frac{2\lambda\tau}{n(2\lambda+\tau)}SI - \gamma I, \tag{2}$$

which in terms of $i = I/k$ (and noting that $S = sk$), becomes

$$\frac{di}{dt} = \frac{2\lambda}{n}\frac{\tau}{2\lambda+\tau}ksi - \gamma i = \beta si - \gamma i, \tag{3}$$

where the rightmost term exhibits the classical SIS form, with $\beta = \frac{2\lambda\tau k}{(2\lambda+\tau)n}$.

4. Protection effect model

We consider the protective behavior induced by how agents elect each next-hop during their random walks. Decisions are made locally, based on information from neighboring nodes only. Yet, agents may not have perfect knowledge about the epidemic state of near locations, or might need to visit such places anyway. Thus, PFx are represented as *biased* random walks: every agent a has its random walk biased so that *hostile nodes*—the ones to yield SI-contacts, should a move into these—are avoided. From the I-agents' perspective, such walks may be considered as to encode their concern on not becoming disease-vectors themselves.

Let w_s and w_i denote S-agents' and I-agents' biases to avoid SI-contacts, respectively, where $0 \leq w_s, w_i \leq 1$. Consider the location of an S-agent j at time t, namely $v = v_j(t) \in V$. When j moves, it no longer chooses among v's neighboring nodes uniformly, but avoids hostile nodes with a bias w_s. Let t now denote the moment at which j walks. The probability that j moves to a node $u \in N(v)$ is

$$\begin{cases} w_s/W_{v,t} & \text{, if there is at least one I-agent in node } u \in N(v) \text{ at } t; \\ 1/W_{v,t} & \text{, otherwise.} \end{cases} \tag{4}$$

where $W_{v,t}$ is the normalizing constant that depends on v and t. In particular, let $H_{u,t}$ denote the event "node $u \in N(v)$ is hostile at time t". Then

$$W_{v,t} = \sum_{u \in N(v)} w_s^{\mathbb{I}(H_{u,t})} \tag{5}$$

where $\mathbb{I}(\cdot)$ is the indicator function. Note that the step probability of the agents now depend on the instantaneous state of neighboring nodes. The PFx of I-agents follows accordingly, substituting w_s for w_i in the above formulation. Thus, the probability that an I-agent at node v moves to $u \in N(v)$ at time t is given by

$$\begin{cases} w_i/W_{v,t} & \text{, if there is at least one S-agent in node } u \text{ at time } t; \\ 1/W_{v,t} & \text{, otherwise.} \end{cases} \tag{6}$$

where $W_{v,t}$ is the appropriate normalizing constant.

Note that when $w_s = w_i = 1$ the model behaves as before (agents choose their next location uniformly), which implies no PFx. Conversely, if $w_s = w_i = 0$ then S-agents (resp. I-) never step into nodes where an I-agent (resp. S-) is made present. This is the strongest possible PFx, which is likely to end any epidemic. Clearly, w_s and w_i may significantly impact the epidemic's outcome, as discussed next.

5. Theoretical analysis

The PFx model proposed is now coupled with the epidemic model presented in Section 3 in order to evaluate key-aspects, namely (i) the SI-contact rate (a fundamental model parameter), (ii) dynamics of infected population, and (iii) the basic reproduction number R_0. Again, the network is assumed to be a complete graph.

5.1. SI-contact rate

The SI-contact rate now depends on the PFx parameters w_s and w_i. This rate can be represented as the sum of two rates: the rate with which S-agents step into locations with I-agents, and vice-versa. These two cases are considered separately, starting with the S-agents, as follows.

Consider an S-agent at the moment it takes a step. The probability it enters a location where an I-agent resides can be computed as follows. Recall that there are I infected agents, each occupying a different location (due to sparsity assumption). Each such location is avoided with bias w_s. There are $n - I$ other locations, each taken with a bias of 1. Thus, the probability that an S-agent provokes an SI-contact is simply

$$p = \frac{Iw_s}{Iw_s + n - I} = \frac{Iw_s}{I(w_s - 1) + n}. \tag{7}$$

Analogously, consider an I-agent at the moment it takes a step. The probability that it enters a location where an S-agent resides can be computed as follows. Recall that there are S susceptible agents, each occupying a different location (due to sparsity assumption). Each such location is avoided with bias w_i. There are $n - S$ other locations, each taken with a bias of 1. Thus, the probability that an I-agent provokes an SI-contact is

$$q = \frac{Sw_i}{S(w_i - 1) + n}. \tag{8}$$

The SI-contact rate will thus depend on the number of S/I-agents walking at rate λ each, and their respective SI-contact probabilities, such that

$$\alpha = \lambda Sp + \lambda Iq = \lambda SI \left(\frac{w_s}{I(w_s - 1) + n} + \frac{w_i}{S(w_i - 1) + n} \right). \tag{9}$$

Note that α is a fundamental parameter for the model, and is the main modification required in the models presented in Section 3.

5.2. Evolution of infectives

Under the PFx perspective, the SI-contact rate from Section 5.1 must be accommodated into the model. Note, however, that the probability σ of contagion remains the same for an SI-contact, as well as the recovery rate γ. Thus, the change in the number of I-agents becomes $dI/dt = \alpha\sigma - \gamma I$, i.e.

$$\frac{dI}{dt} = \frac{\tau\lambda}{2\lambda + \tau} \left(\frac{w_s}{I(w_s - 1) + n} + \frac{w_i}{S(w_i - 1) + n} \right) SI - \gamma I. \tag{10}$$

We may rewrite Equation 10 in terms of $i = I/k$ and s, noting that $S = sk$. Thus

$$\frac{di}{dt} = \frac{\tau\lambda k}{2\lambda + \tau} \left(\frac{w_s}{i(w_s - 1) + n} + \frac{w_i}{sk(w_i - 1) + n} \right) si - \gamma i \tag{11}$$

wherein the infection rate β now becomes dependent on i, such that

$$\beta(i) = \frac{\tau\lambda k}{2\lambda + \tau} \left(\frac{w_s}{i(w_s - 1) + n} + \frac{w_i}{sk(w_i - 1) + n} \right) \tag{12}$$

and hence $di/dt = \beta(i)si - \gamma i$. Note, however, that β's dependence on i is actually negligible. Indeed, $-1 \leq i(w_s - 1) \leq 0$, and hence $i(w_s - 1) + n \approx n$. Likewise, the premise of sparsity imposes $k \ll n$, and consequently $sk(w_i - 1) + n \approx n$. Therefore, a good approximation for Equation 12 is

$$\beta = \frac{\tau\lambda k(w_s + w_i)}{(2\lambda + \tau)n}, \tag{13}$$

and for the particular case wherein $w_s = w_i = w$, Equation 13 becomes

$$\beta = \frac{2\tau\lambda kw}{(2\lambda + \tau)n}. \tag{14}$$

Finally, rewriting Equation 11 in terms of Equation 13 gives

$$\frac{di}{dt} = \frac{\tau\lambda k(w_s + w_i)}{(2\lambda + \tau)n}si - \gamma i\,. \tag{15}$$

5.3. Reproduction number

The basic reproduction number $R_0 = \beta/\gamma$ is a classical metric which considers the pathogen's capacity of spreading, and is used to indicate whether the epidemic will die out shortly ($R_0 < 1$) or long-last among population ($R_0 > 1$) [Newman 2010]. Within the context of PFx, a natural question arises: is there a range of values for w_s and w_i as a function of other model parameters that ensures $R_0 < 1$? In order to answer, let us first consider a constant C defined as

$$C = \frac{\tau k\lambda}{(2\lambda + \tau)n} \tag{16}$$

so that $\beta = C(w_s + w_i)$ when $w_s \neq w_i$, and $\beta = 2Cw$ when $w_s = w_i = w$. Trivially, $2C/\gamma < 1 \implies R_0 < 1$ for any $\{w_s, w_i\}$, i.e. the epidemic is led to extinction even in the absence of protective efforts. Conversely, if $2C/\gamma \geq 1$, then

$$R_0 < 1 \iff \frac{\beta}{\gamma} < 1 \iff \frac{C(w_s + w_i)}{\gamma} < 1 \iff w_s + w_i < \frac{\gamma}{C}, \tag{17}$$

and for the particular case wherein $w_i = w_s = w$,

$$R_0 < 1 \iff w < \gamma/2C. \tag{18}$$

Equation 17 exposes that both w_s and w_i, alone, deliver limited protection in the case the other assumes a fixed value. For instance, if infected agents induce no protection ($w_i = 1$) then $R_0 < 1 \implies w_s < (\gamma - C)/C$, which is not possible when $\gamma - C < 0$ since $0 \leq w_s \leq 1$. On the other hand, Equation 18 shows that there always exists some $w > 0$ that forces $R_0 < 1$, i.e. the S/I-agents joint engagement may positively prevent endemic steady-states. Note, however, that the value for w to satisfy Equation 18 depends on both λ and τ. A particularly interesting question is thus whether there exists a regime for w under which $R_0 < 1$ *even in the case* λ (resp. τ) *is arbitrarily large*, for a fixed τ

(resp. λ). This regime can be identified by considering the asymptotic behavior of λ and τ, one at a time, on the infection rate β (Equation 14). Indeed,

$$\lim_{\lambda\to\infty}\beta = \lim_{\lambda\to\infty}\frac{2\tau\lambda kw}{(2\lambda+\tau)n} = \frac{\tau kw}{n} = \beta^{'}, \tag{19}$$

which yields a basic reproduction number $R_0^{'} = \beta^{'}/\gamma$. Clearly, $\beta^{'} < \gamma \implies R_0 < 1$. Thus,

$$R_0 < 1 \iff w < \frac{\gamma n}{\tau k}. \tag{20}$$

Interestingly, any w satisfying Equation 20 will manage to extinguish the epidemic irrespective of the walk rate. Indeed, larger walk rates, on the one hand, increase SI-contacts per unit time; on the other, they reduce the S-agents' exposition time as well. In similar fashion, as $\tau \to \infty$ (for a fixed λ), β converges to $\beta^{'} = (2\lambda kw)/n$. Here, $\beta^{'} < \gamma$ is met case $w < (\gamma n)/(2\lambda k)$.

6. Numerical results

In what follows we present simulation results that validate the theoretical analysis from Section 5. A discrete-event simulator [Ross 2013] was designed and implemented [de Souza 2020] in order to generate performance metrics concerning the impacts of PFx and other model parameters. All results to follow assume $i_0 = 0.5$ and simulation time limit $T = 10^5$.

Figure 1(a) shows the fraction of infected agents over time for different levels of PFx. Each given w yields two different curves in the plot: the numerical simulation from one single run and the model prediction, as in Equation 15. Note that the model succeeds in capturing the average dynamics for each protection level. Moreover, the value for w decisively changes the epidemic's outcome. In particular, the protective level $w = 0.14$ has managed to hinder the epidemic, leading to a disease-free steady state in a short time. Indeed, from the given parameters, and from Equation 18, $w = 0.14 < \gamma/2C = 0.1425$, thus implying $R_0 < 1$.

Figure 1(b) shows how R_0 varies as a function of w for two different population sizes, namely $k = 400$ and the 5x-larger $k = 2000$. Note that R_0 grows linearly for both cases, but has higher slope when k is larger. The point highlighted in green—for which R_0 is slightly below 1—indicates the protective level of $w = 0.14$ shown in Figure 1(a).

The epidemic's average duration in function of k and λ are shown in figures 2(a) and 2(b), respectively. Each dot from each curve averages upon 30 runs. For the simulation time limit being fixed at $T = 10^5$, such average is made over two possibilities for each run: (i) the epidemic being finished at $t < T$ (thus $|S(t)| = k$), or (ii) the time limit T being reached. Each curve refers to a different epidemic scenario, in terms of either the network size n and the protection level w. Note that to increase either k or λ leads to a phase transition on the epidemic duration (from ephemeral to long-lasting). More importantly, Figure 2(a) illustrates how PFx may drastically increase the epidemic threshold. In particular, by comparing the two epidemics for $n = 10^5$, note that $w = 0.6$ right-shifts the phase transition observed for $w = 1$ (starting around $k = 300$) by approximately 200 agents. This means that upon increasing risk avoidance by 40%—by changing the

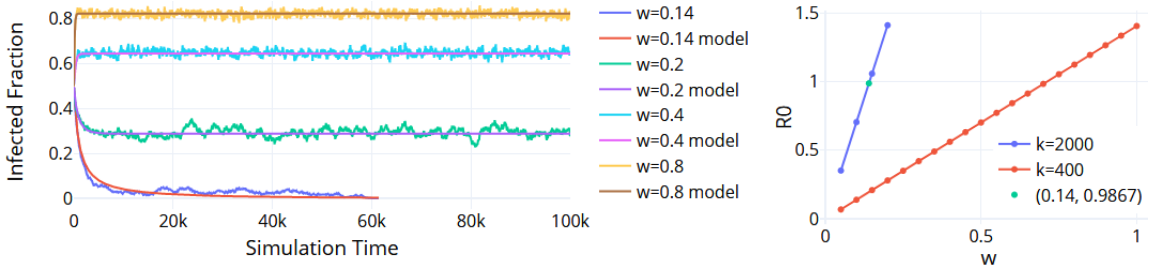

(a) Fraction of infected agents over time ($k = 2000$).

(b) Basic reproduction number as a function of w.

Figure 1. Fraction of infected agents as a function of time for different scenarios (left), and the reproduction number R_0 (right) as a function of w when $k = \{400, 2000\}$. For both figures, $\tau = 1; \gamma = 1.9 \cdot 10^{-3}; \lambda = 1$; $n = 10^5$.

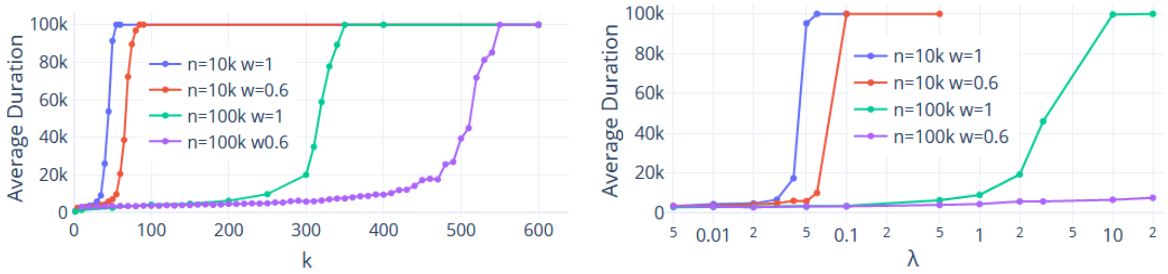

(a) Average duration of different epidemics in function of k ($\lambda = 1$).

(b) Average duration of different epidemics in function of λ (x-axis log-scaled; $k = 250$).

Figure 2. Average duration of different epidemics in function of the number k of agents (left) and the walk rate λ (right). For both figures, $\tau = 1; \gamma = 1.9 \cdot 10^{-3}$.

behavior from fully-tolerant ($w = 1$) to 60% tolerant ($w = 0.6$)—the system has managed to preclude epidemic outbreaks for a population about 67% larger (from $k = 300$ to $k = 500$).

Figure 2(b) (x-axis log-scaled) illustrates the impact of the walk rate λ on an epidemic's average duration. Note that 3 out of the 4 curves show scenarios wherein an increase in the walk rate leads to a phase transition (very long duration). In turn, for the curve "$n = 10^5, w = 0.6$" the duration increases slowly even when λ reaches 20. It could be the case of a phase transition still being reached for some even larger λ. However, from Equation 19, as $\lambda \to \infty$ the infection rate β converges to $\beta' = (\tau k w)/n$. For the given parameters, it yields a basic reproduction number $R_0' = \beta'/\gamma = 0.0015/0.0019 = 0.79 < 1$. This means that the protective level of $w = 0.6$ will manage to impede long-lasting epidemics *upon any walk rate* λ, in sharp contrast with the scenario where $w = 1$.

7. Conclusion

This work proposed and analysed a parsimonious PFx model for network epidemics with random walks. The simple model uses biases in random walk mobility to embody protection from both S-agents and I-agents. Through ODE-based analysis, we have identified key-aspects from the resultant dynamics, such as the average number of infected agents over time. It has also been shown the connection of our model to the classical

SIS, with fundamental predictions being provided. In particular, we have identified the risk-avoidance regime under which the epidemic vanishes irrespective of either the walk rate and the transmissibility rate.

While the analyses in this paper have focused on complete graphs, the proposed model can contribute to further investigations of PFx upon network epidemics with mobile agents. Indeed, the relationship between network structure and the influence of PFx is a natural theme for future investigation.

References

[Amante and Balmer 2020] Amante, A. and Balmer, C. (2020). Italy in coronavirus lockdown as deaths soar and economy fades. Accessed: 2020-03-11.

[Cai et al. 2015] Cai, Y., Kang, Y., Banerjee, M., and Wang, W. (2015). A stochastic sirs epidemic model with infectious force under intervention strategies. *Journal of Differential Equations*, 259(12):7463 – 7502.

[Capasso and Serio 1978] Capasso, V. and Serio, G. (1978). A generalization of the kermack-mckendrick deterministic epidemic model. *Mathematical Biosciences*, 42(1):43 – 61.

[Cauchemez et al. 2011] Cauchemez, S., Bhattarai, A., Marchbanks, T., Fagan, R., Ostroff, S., Ferguson, N., and Swerdlow, D. (2011). Role of social networks in shaping disease transmission during a community outbreak of 2009 h1n1 pandemic influenza. *PNAS*, 108:2825–30.

[de Souza 2020] de Souza, R. C. (2020). Simulator for network epidemics with biased random walks as protection effects. `https://github.com/rchiesse/randomWalk`.

[Draief and Ganesh 2011] Draief, M. and Ganesh, A. (2011). A random walk model for infection on graphs: Spread of epidemics & rumours with mobile agents. *Discrete Event Dynamic Systems*, 21(1):41–61.

[Eames et al. 2012] Eames, K. T. D., Tilston, N. L., Brooks-Pollock, E., and Edmunds, W. J. (2012). Measured dynamic social contact patterns explain the spread of h1n1v influenza. *PLOS Computational Biology*, 8(3):1–8.

[Funk et al. 2010] Funk, S., Salathé, M., and Jansen, V. (2010). Modelling the influence of human behaviour on the spread of infectious diseases: A review. *Journal of the Royal Society, Interface / the Royal Society*, 7:1247–56.

[Granell et al. 2013] Granell, C., Gómez, S., and Arenas, A. (2013). Dynamical interplay between awareness and epidemic spreading in multiplex networks. *Phys. Rev. Lett.*, 111:128701.

[Guo et al. 2018] Guo, W., Cai, Y., Zhang, Q., and Wang, W. (2018). Stochastic persistence and stationary distribution in an sis epidemic model with media coverage. *Physica A: Statistical Mechanics and its Applications*, 492:2220 – 2236.

[Hyman and Li 1997] Hyman, J. M. and Li, J. (1997). Behavior changes in sis std models with selective mixing. *SIAM Journal on Applied Mathematics*, 57(4):1082–1094.

[Ibrahim 2012] Ibrahim, P. S. Y. (2012). Modelagem e Análise de Epidemias SIS em Redes baseadas em Passeios Aleatórios. Master's thesis, Federal University of Rio de Janeiro, Brazil.

[Lam et al. 2012] Lam, H., Liu, Z., Mitzenmacher, M., Sun, X., and Wang, Y. (2012). Information dissemination via random walks in d-dimensional space. SODA '12, page 1612–1622, USA. Society for Industrial and Applied Mathematics.

[Lee et al. 2012] Lee, S., Rocha, L. E. C., Liljeros, F., and Holme, P. (2012). Exploiting temporal network structures of human interaction to effectively immunize populations. *PLOS ONE*, 7(5):1–10.

[Mao and Yang 2012] Mao, L. and Yang, Y. (2012). Coupling infectious diseases, human preventive behavior, and networks – a conceptual framework for epidemic modeling. *Social Science & Medicine*, 74(2):167 – 175.

[Newman 2010] Newman, M. (2010). *Networks: An Introduction*. Oxford University Press, Inc., USA.

[Ogilvy et al. 1927] Ogilvy, K. W., G., M. A., and Thomas, W. G. (1927). A contribution to the mathematical theory of epidemics. *Proc. R. Soc. Lond. A*, 115.

[Robinson et al. 2007] Robinson, S., Everett, M., and Christley, R. (2007). Recent network evolution increases the potential for large epidemics in the british cattle population. *Journal of the Royal Society, Interface / the Royal Society*, 4:669–74.

[Ross 2013] Ross, S. (2013). Chapter 7 - the discrete event simulation approach. In *Simulation*, pages 111 – 134. Academic Press.

[Tavares 2018] Tavares, J. V. B. (2018). Simulação Escalável de Epidemias SIS Baseadas em Passeios Aleatórios com Caracterização de Transições de Fase. Master's thesis, Federal University of Rio de Janeiro, Brazil.

[Tchuenche et al. 2011] Tchuenche, J., Dube, N., Bhunu, C., Smith, R., and Bauch, C. (2011). The impact of media coverage on the transmission dynamics of human influenza. *BMC public health*, 11 Suppl 1:S5.

[Volz and Meyers 2007] Volz, E. and Meyers, L. (2007). Susceptible-infected-recovered epidemics in dynamic contact networks. *Proceedings. Biological sciences / The Royal Society*, 274:2925–33.

[Wang et al. 2015] Wang, Z., Andrews, M. A., Wu, Z.-X., Wang, L., and Bauch, C. T. (2015). Coupled disease–behavior dynamics on complex networks: A review. *Physics of Life Reviews*, 15:1 – 29.

[Yang et al. 2018] Yang, H.-X., Tang, M., and Wang, Z. (2018). Suppressing epidemic spreading by risk-averse migration in dynamical networks. *Physica A: Statistical Mechanics and its Applications*, 490:347 – 352.

[Zhang et al. 2015] Zhang, Z., Wang, H., Wang, C., and Fang, H. (2015). Modeling epidemics spreading on social contact networks. *IEEE Transactions on Emerging Topics in Computing*, 3(3):410–419.

[Zhou et al. 2012] Zhou, J., Xiao, G., Cheong, S. A., Fu, X., Wong, L., Ma, S., and Cheng, T. H. (2012). Epidemic reemergence in adaptive complex networks. *Phys. Rev. E*, 85:036107.